https://doi.org/10.5194/gmd-2021-2
Preprint. Discussion started: 11 March 2021

Geoscientific Model Development Discussions
Open Access
EGU

S2P3-R v2.0: computationally efficient modelling of shelf seas on regional to global scales

Paul R. Halloran[1], Jennifer K. McWhorter[1,2], Beatriz Arellano Nava[1], Robert Marsh[3], William Skirving[4,5]

[1]College of Life and Environmental Sciences, University of Exeter, Exeter, UK
[2]School of Biological Sciences, The University of Queensland, Brisbane, Queensland, Australia
[3]University of Southampton, National Oceanography Centre, Southampton, UK
[4]Coral Reef Watch, National Oceanic and Atmospheric Administration, College Park, MD, USA
[5]ReefSense Pty Ltd, Cranbrook, Queensland, Australia

Correspondence to: Paul R. Halloran (p.halloran@exeter.ac.uk)

Abstract. The marine impacts of climate change on our societies will be largely felt through coastal waters and shelf seas. These impacts involve sectors as diverse as tourism, fisheries and energy production. Projections of future marine climate change come from global models. Modelling at the global scale is required to capture the feedbacks and large-scale transport of physical properties such as heat, which occur within the climate system, but global models currently cannot provide detail in the shelf-seas. Version 2 of the regional implementation of the Shelf Sea Physics and Primary Production (S2P3-R v2.0) model bridges the gap between global projections and local shelf-sea impacts. S2P3-R v2.0 is a highly simplified coastal shelf model, computationally efficient enough to be run across the shelf seas of the whole globe. Despite the simplified nature of the model, it can display regional skill comparable to state-of-the-art models, and at the scale of the global (excluding high-latitudes) shelf-seas can explain >50% of the interannual SST variability in ~60% of grid cells, and >80% of interannual variability in ~20% of grid cells. The model can be run at any resolution for which the input data can be supplied, without expert technical knowledge, and using a modest off-the-shelf computer. The accessibility of S2P3-R v2.0 places it within reach of an array of coastal managers and policy makers. S2P3-R v2.0 is set up to be driven directly with output from reanalysis products or daily atmospheric output from climate models such as those which contribute to the 6th phase of the Climate Model Intercomparison Project, making it a valuable tool for semi-dynamical downscaling of climate projections. The updates introduced into version 2.0 of this model are primarily focused around the ability to geographical relocate the model, model usability and speed, but also scientific improvements. The value of this model comes from its computational efficiency, which necessitates simplicity. This simplicity leads to several limitations, which are discussed in the context of evaluation at regional and global scales.

1. Introduction

The world's coastal oceans are under increasing pressure from human activity (Doney, 2010). These shallow, relatively accessible waters are where humans interact most with the ocean, and where marine biological activity and diversity are often at their most intense (Mora *et al.*, 2013; Bowen *et al.*, 2016). Global Circulation and Earth System Model projections contain neither the spatial resolution nor processes required to simulate shelf seas (Holt *et al.*, 2009). These models have been found to contain little to no skill at simulating patterns of surface

https://doi.org/10.5194/gmd-2021-2
Preprint. Discussion started: 11 March 2021

Geoscientific Model Development Discussions

temperature warming at spatial scales lower than 1000km (Kwiatkowski *et al.*, 2014). While at regional scales shelf-sea models are providing extremely valuable information over short time horizons (e.g. Steven *et al.*, 2019), the state-of-the-art in shelf-sea climate projections is either to downscale global models over small regions using complex 3D shelf sea models (e.g. Tinker and Howes, 2020) at considerable computational expense, or downscale large-scale projections statistically (e.g. Donner *et al.*, 2005; Van Hooidonk *et al.*, 2016). S2P3-R v2.0 aims to bridge the gap between high-complexity small scale projections, and large-scale statistical projections which ignore local processes and dynamics.

The underlying physical-biological model used in S2P3-R is the Shelf Sea Physics and Primary Production (S2P3) model (Simpson and Sharples, 2012). S2P3 makes the common assumption that in many regions variability on the shelf is dominated by atmospheric and tidal processes rather than by communication with the open ocean (e.g. Song *et al.*, 2011; van der Molen, Ruardij and Greenwood, 2017), and consequently, represents the ocean at a location as a 1D column of water. The physical and biological components of S2P3 are discussed below, but are described in further detail in Simpson and Sharples (2012), Sharples et al. (2006), Sharples (2008) and summarised in Marsh et al., (2015). S2P3-R v1.0 (Marsh, Hickman and Sharples, 2015) placed S2P3 into a spatial framework by representing the shelf sea as a 2D array of neighbouring independent 1D columns of water. S2P3-R v2.0 addresses several the limitations in S2P3-R v1.0, which prevented it from being used effectively to downscale large-scale reanalyses or climate projections.

2. Overview of the underlying 1D model, S2P3

S2P3-R v2.0 is the 2nd generation of regional-model development building on the 1D shelf sea model S2P3 (Sharples *et al.*, 2006). The physical component of S2P3 simulates vertical profiles of temperature, turbulence and currents in response to tidal and wind driven mixing. The model calculates the tidal slope from the prescribed M2, S2, N2, O1 and K1 tidal ellipses, and from this, the water's velocity (Sharples *et al.*, 2006). The stress applied by the tides is then calculated as a function of the velocity at 1m above the seabed, the density of the seawater and a prescribed bottom drag coefficient (Sharples *et al.*, 2006). The surface stress exerted by the wind is calculated as a function of windspeed and direction (with respect to tides), air pressure and a windspeed-dependent surface drag coefficient (Smith and Banke, 1975). A turbulence closure scheme calculates profiles of vertical eddy viscosity and diffusivity as a function of current shear and vertical density (Canuto *et al.*, 2001). The surface and bottom stress are propagated through the water column as a function of the vertical eddy viscosity, which is derived from the turbulence closure scheme (Sharples *et al.*, 2006). S2P3 considers only the role of temperature, not salinity, on density (Sharples *et al.*, 2006), limiting its application in cold water (where density variations are dominated by salinity), or variable salinity settings such as near river outflows.

The biological model in S2P3 takes a lightweight and pragmatic view of representing primary production. Phytoplankton concentrations are modelled as a function of their initial concentration, vertical mixing, growth rate and a fixed grazing rate (Sharples, 2008). Phytoplankton growth rate is a function of the maximum growth rate for a given temperature and nutrient availability, modified by available photosynthetically active radiation

https://doi.org/10.5194/gmd-2021-2
Preprint. Discussion started: 11 March 2021

(PAR) and maximum light utilisation rate, minus respiration at a constant rate (Sharples, 2008). Surface PAR is set to 45% of the net downwelling surface shortwave radiation, and this decays as a function of phytoplankton concentration and an attenuation coefficient which is dependent on whether the water column is mixed or stratified (Sharples, 2008). Nutrient availability is a function of vertical mixing, uptake by phytoplankton and loss through grazing, and is restored towards a constant concentration in the lowest model level (Sharples, 2008). The simple assumptions made within the biological model align with the desire to keep the computational cost of the model low, but also to avoid including poorly constrained processes within the model (Sharples, 2008). These simplifications and their impacts are discussed further in Sharples (2008). In its original form S2P3 was driven by sinusoidal timeseries of surface air temperature and pressure, relative humidity, total cloud cover and u and v surface winds.

3. Scientific advances from S2P3

Version 1 of S2P3-R modified the S2P3 code and provided bash scripts to run S2P3 as a 2D array of 1D column models to provide a computationally efficient way to simulate shelf sea physical and biological conditions (Marsh, Hickman and Sharples, 2015). Application of this version of the model demonstrated that this simple approach to shelf-sea modelling produced sensible patterns of temperature, stratification and primary production on the North West European Shelf and East China and Yellow seas, and showed that the model reproduced observed year to year variability at two sites in the English Channel (Marsh, Hickman and Sharples, 2015). The success of S2P3-R at reproducing physical and biological structures over the recent past has motivated the developments and evaluation presented here. The developments described here are aimed at running the model at larger spatial scales and over longer time periods, including into the future to downscale and explore the coastal implications of future climate change. These developments presented several practical challenges, which are discussed below.

S2P3-R v1.0 introduced spatial information into its simulation by considering local bathymetry and tidal mixing, as well as a latitudinal dependence of the clear-sky radiation and Coriolis parameter used within the model (Marsh, Hickman and Sharples, 2015). Application of the model over larger spatial domains was limited scientifically because it used common timeseries of surface air temperature and pressure, relative humidity, cloud fraction and wind velocities to drive all water columns within a simulation. S2P3-R v2.0 addresses this limitation by utilising meteorological timeseries specific to each grid location which are generated from reanalysis or climate models using the provided scripts (see below and the Code Availability section).

Previous iterations of the model have represented downwelling shortwave irradiance as a function of time of year, latitude and total cloud fraction. While this approach has been applied successfully when considering the North West European Shelf (Sharples *et al.*, 2006; Sharples, 2008; Marsh, Hickman and Sharples, 2015), total cloud fraction cannot account for the impacts on radiation of moving between regions of different cloud type or changes in cloud microphysics. Over climate timescales, changes in aerosol emissions, meteorology and atmospheric chemistry will have considerable impacts on the shortwave radiation received at the sea surface (Haywood and Boucher, 2000), which may dominate greenhouse gas driven climate signals at regional scales (Booth *et al.*, 2012).

https://doi.org/10.5194/gmd-2021-2
Preprint. Discussion started: 11 March 2021

Geoscientific Model Development Discussions

S2P3-R v2.0 moves to prescribing the net downwards surface radiation explicitly from the reanalysis product or climate model output from which it is driven.

Analogous to the treatment of shortwave radiation within S2P3, the net loss of heat from the surface of the ocean in the form of longwave radiation was calculated in S2P3-R v1.0 from the temperature-dependent longwave emission derived from the Stefan–Boltzmann equation, moderated by cloud-fraction and humidity. This approach cannot account for spatial/temporal changes in cloud-top height and optical thickness, which have been shown to be as important as cloud fraction in determining the radiation field (Chen, Rossow and Zhang, 2000). These factors are of 1st order importance when relocating the model from high to low latitudes, performing simulations spanning these latitudes, or when considering the impacts of anthropogenic aerosols and cloud-feedbacks in response to climate change. A further limitation of inferring the downwelling longwave radiation as a function of cloud fraction when performing long historical simulations or simulations driven from future climate projections, is that the change in the radiation budget associated with changing greenhouse gas concentrations is not directly accounted for. S2P3-R v2.0 revises the surface heat-loss through longwave radiation ($Q_{LongwaveNet}$) to:

$$Q_{LongwaveNet} = \varepsilon_{longwave}\sigma T^4 - Q_{LongwaveDownwards}S \quad (1)$$

Where $\varepsilon_{longwave}$ is the long-wave emissivity (0.985), σ is the Stefan–Boltzmann constant ($\sigma = 5.67 \times 10^{-8}$ W m^{-2} K^{-4}), T is the temperature of the surface layer, $Q_{LongwaveDownwards}$ is the prescribed downwelling longwave radiation at the surface, and S is a constant to account for the fact that the model is not simulating the ocean skin, where a proportion of the longwave radiation will be absorbed and re-emitted without interacting with the water at the depths represented by the top layer of the model.

To facilitate longer timesteps in deeper waters, S2P3-R v1.0 scaled the vertical resolution in each water column with the water-depth. This has been revised to a fixed 2m vertical resolution in S2P3-R v2.0 to prevent variability in level thickness introducing spatial artefacts to simulated surface water conditions. Phytoplankton growth in the model, and therefore primary production relies on a flux of nitrate into the lowest vertical level of the model. In S2P3-R v2.0 we move from representing this as a single value in space and time, to a value specific to each grid box, read in from an ancillary file. A script is provided to generate this ancillary file from World Ocean Atlas (Levitus, 1982) data (see Code Availability section).

A schematic overview of S2P3-R v2.0 is presented in Figure 1.

https://doi.org/10.5194/gmd-2021-2
Preprint. Discussion started: 11 March 2021

Geoscientific Model Development Discussions

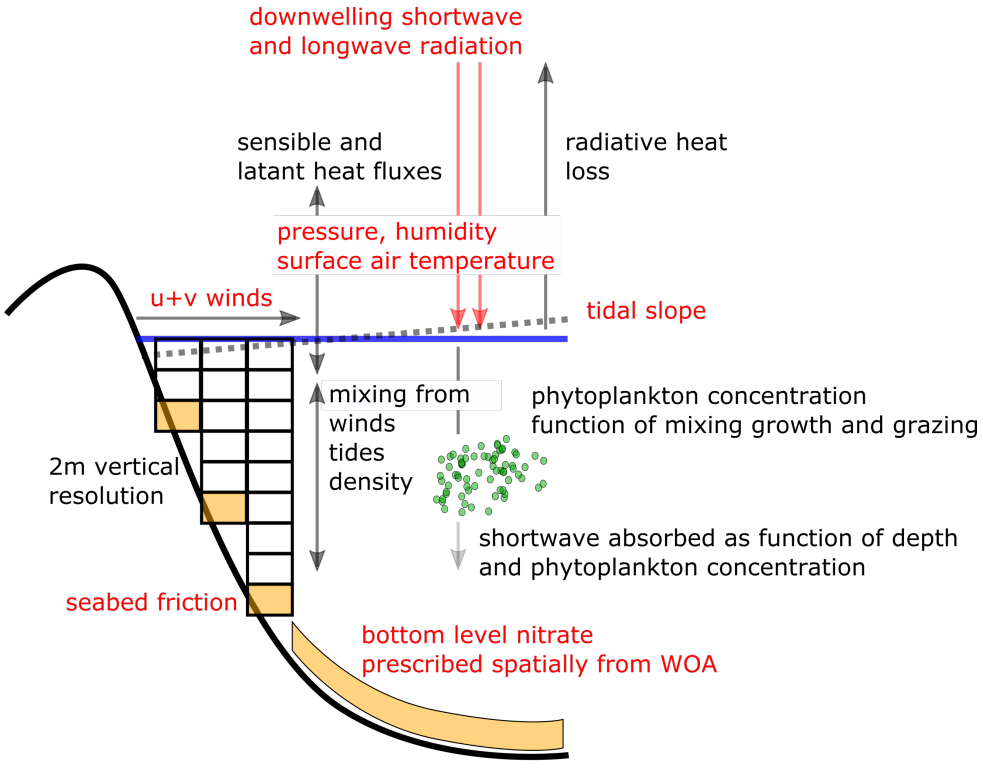

Figure 1. Schematic description of the processes accounted for in S2P3-R v2.0 and prescribed quantities, both forcings and constants. WOA stands for World Ocean Atlas.

4. Practical advances from S2P3

The practical developments made to version 2.0 of S2P3-R fall into two categories (1) how the model runs, and (2) how to generate the data used to set up and force the model.

The initial spatial implementation of S2P3 (S2P3-R v1.0) focused on what could be achieved by running S2P3 in a regional sense, and as such provided Bash scripts which ran individual instances of the 1D model for each of the latitude/longitude locations specified in a domain file containing depth and tidal forcing data. S2P3-R v2.0 makes several changes to reduce the amount of input-output associated with this approach and distributes the processing of water columns over multiple processor cores. This is done by (1) re-writing the code which runs the underlying Fortran model code from Bash to Python using the multiprocessing module, (2) reading the depth and tidal data from file once, then passing it from memory to the Fortran code for each point, and (3) accumulating the output annually and writing this year by year to netCDF or text files. The model has been modified to run one year at a time, writing output then 'resubmitting' to allow long, high-resolution, or large spatial domain, simulations to be performed without hitting memory or submission length limits.

https://doi.org/10.5194/gmd-2021-2
Preprint. Discussion started: 11 March 2021

Geoscientific Model Development Discussions

The independence of each grid point, combined with the developments to consolidate reading or writing data to disk, means that the model scales very efficiently when more/fewer processor cores are used (Figure 2).

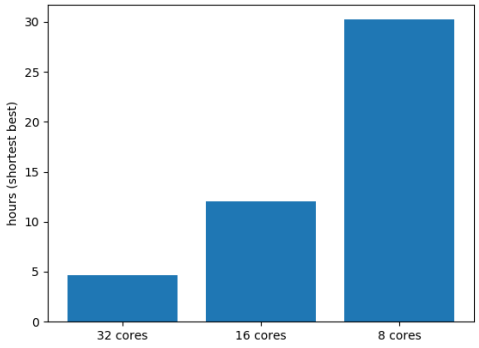

Figure 2. Processing time in hours to complete one year of simulation at 0.2º resolution in a 'global' (65ºS-65ºN, 180ºW-180ºE) configuration spanning water depths of 10-100m. The high latitudes were removed because the model assumes constant salinity and the model does not include a representation of sea ice. Simulations were undertaken on an AMD 2990WX 32-Core 3Ghz Processor with multi-threading.

Model developments around usability include (1) translating the Fortran code so it can be compiled with the open-source GFortran compiler rather than the proprietary ifort compiler and by doing so improving accessibility, (2) providing the user-option to generate output files directly in netCDF format, (3) providing an interface for prescribing which output diagnostics the user wishes to produce, and (4) the provision of scripts and associated ReadMe files to enable simple generation of all of the required input files (see Code Availability section). These files are the domain (which specify the depth and tidal forcing for each model grid-point), nutrient ancillary and meteorological forcing files (Figure 3). The input generation scripts, the input data they require, and how the outputs are used by the main model are detailed in Figure 3. The practicalities of how to obtain and run the scripts and associated data are detailed in the code availability section and supplied ReadMe files (see Code Availability section).

https://doi.org/10.5194/gmd-2021-2
Preprint. Discussion started: 11 March 2021

Geoscientific Model Development Discussions
Open Access
EGU

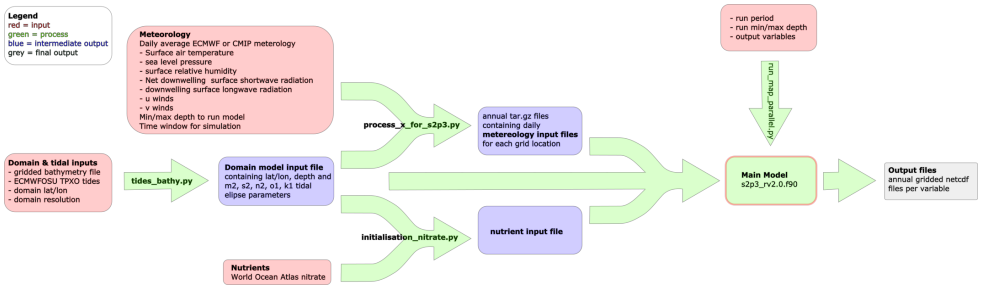

Figure 3. Overview of the S2P3-R v2.0 framework, which includes the model and runscript but also separate scripts to generate the required input files. The arrows show where externally available data or the output from one component of S2P3-R V2.0 is supplied to another component/output.

5. Global Evaluation

S2P3-R v2.0 is an intentionally simple model. By ignoring lateral advection, one should expect to see model temperature biases in regions of heat convergence or divergence, i.e. where significant amounts of heat are imported or exported through advection, or local dissipation rates are enhanced through horizonal processes. The fact that a region may experience a temperature bias does not itself mean the model is not useful in that region. Despite biases in average temperatures, the model may still capture variability on the timescales of interest. The model variability may however be compromised if there is a temperature bias at low ambient temperatures, where the non-linearity of the equation of state of seawater reduces the sensitivity of density to temperature variability. This limits the applicability of S2P3-R v2.0 in cold waters, and alongside the specification of constant salinity and omission of sea ice processes, means that the evaluation of the model has been restricted to the subpolar and lower latitude ocean (<65ºN/S). The evaluation presented here is intended to allow potential model users to identify whether S2P3-R v2.0 is an appropriate tool to use for the question and location they are interested in. We first evaluate the global performance of the model, then focus evaluation on a mid-latitude, then a low-latitude region. Evaluation in each section begins with the physical variables, then moves on to the biological component of the model.

The model simulations presented here have been set up at 0.2º spatial resolution using the input fields described in table 1.

Table 1. Model inputs.

Model input	Source	Reference
Bathymetry Global and N.W. European Shelf	ETOPO1	(Amante and Eakins, 2009)
Bathymetry Australia	3DGBR	(Beaman, 2010)

https://doi.org/10.5194/gmd-2021-2
Preprint. Discussion started: 11 March 2021

Geoscientific Model Development Discussions

Tides	Produced using the Oregon State University Tidal Inversion Software (OTPS)	(Egbert and Erofeeva, 2002)
Meteorological Forcing	ECMWF ERA5	(Hersbach *et al.*, 2019)
Nutrients	World Ocean Atlas 13	(Levitus, 1982)

5.1 Global Physical Evaluation

An initial comparison of model SSTs against satellite SSTs (Merchant *et al.*, 2019) at a global scale indicates that the model displays its smallest biases in the subtropics to subpolar regions (Figure 4). The prevalence of warm biases in the tropics and cool biases in the high latitudes is consistent with export and import or warm waters from and to these regions respectively (Figure 4). To allow potential users to examine model performance in their regions of interest in greater detail, the data underlying Figure 4 is made available as described in the Data Availability section.

https://doi.org/10.5194/gmd-2021-2
Preprint. Discussion started: 11 March 2021

Geoscientific Model Development Discussions
Open Access
EGU

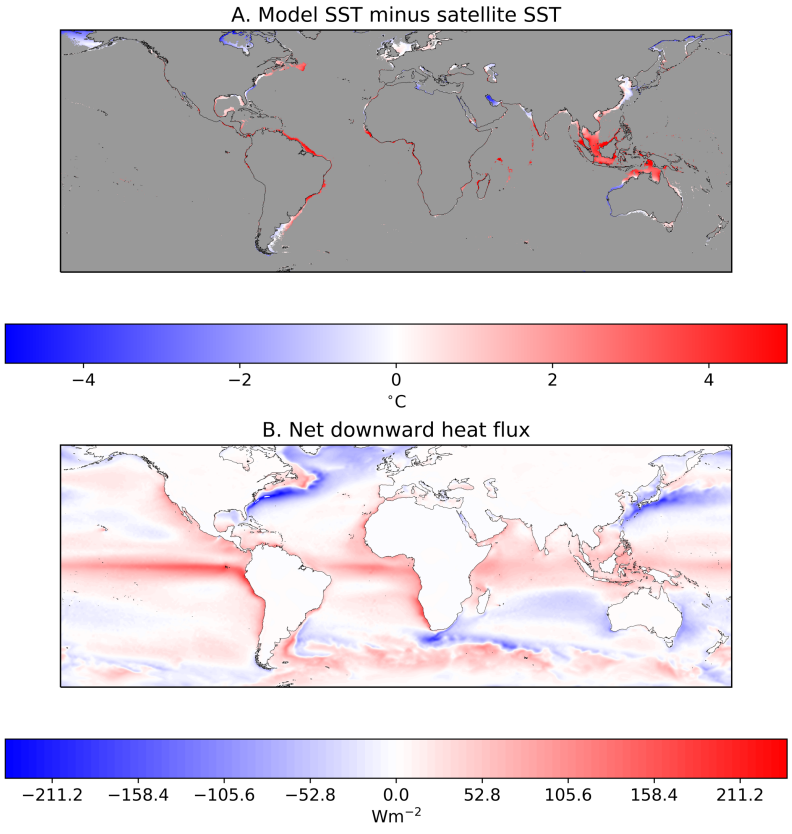

Figure 4. A. Model SST simulation minus satellite SST data averaged between 1st Jan 2006 and 31st Dec 2016. White indicates that the model is displaying no surface temperature bias, red indicates the model displays a warm bias, and blue the model displays a cool bias. The model was forced with atmospheric data from ERA5 (Hersbach et al., 2019). B. Net surface downward heat flux calculated from the ECMWF ERA5 reanalysis (Hersbach et al., 2019). Where this is positive there is a net heat flux into the ocean, and therefore assuming the system is approximately at steady state, advection of heat out of this area. Where the net downward heat flux is negative there is advection of heat into this region. S2P3-R V2.0 does not account for lateral advection, so one would anticipate that the model will display a warm bias in regions where heat is typically advected from (i.e. tropics) and cool biases where heat is advected to (i.e. high latitudes).

Beyond calculating the surface heat budget based on atmospheric forcings, the model skill in simulating surface temperatures comes from vertical mixing processes which exchange heat between the surface and subsurface layers as a function of temperature induced density differences and wind and tide stress. In line with this, we find that large SST biases are more prevalent at low tidal amplitudes (Figure 5). While this analysis indicates that strong tidal mixing can contribute to a skilful simulation, it does not appear that tidal magnitude provides a rule to determine where best to use this model. Stratification is highly seasonal in the mid-latitudes, with stratification typically corresponding to weak tidal mixing in the summer, and a pervasive loss of stratification during the

https://doi.org/10.5194/gmd-2021-2
Preprint. Discussion started: 11 March 2021

Geoscientific Model Development Discussions
Open Access
EGU

winter. If strong tides played a 1st order role in model skill, one would expect to see smaller model biases in the summer than winter across the mid-latitudes (Figure 6).

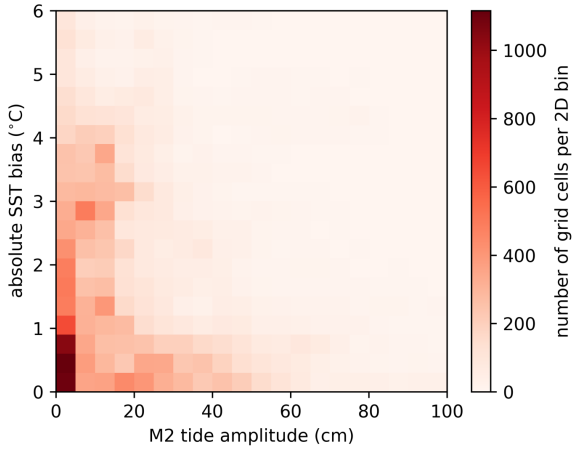

Figure 5. 2D histogram demonstrating the relationship between tidal amplitude (M2 tide) and absolute annual-mean SST difference between the model and satellite data.

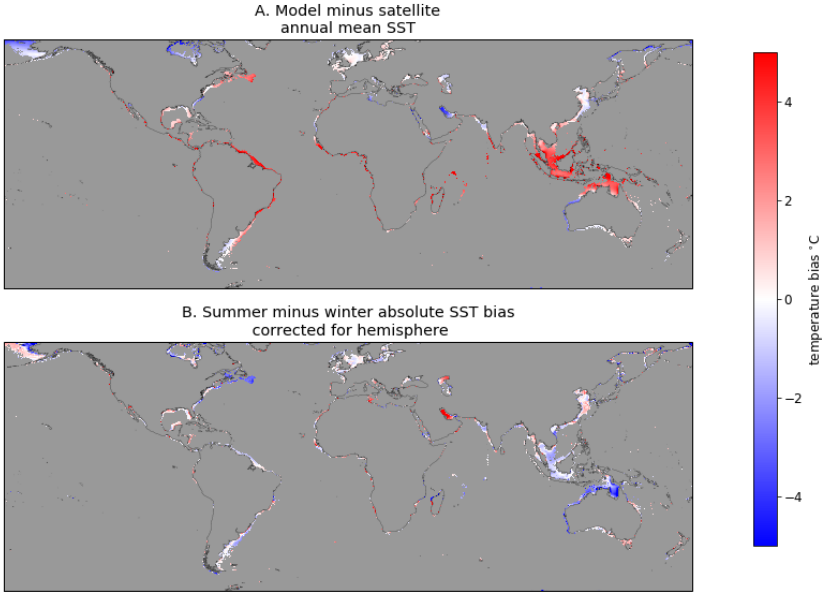

Figure 6. Annual mean SST bias (top), and difference in absolute SST bias between summer and winter (bottom). In (b) Blue indicates that the summer months (June, July, August in the Northern hemisphere and December, January, February in the Southern hemisphere) display a smaller absolute bias than the winter months (December, January, February in the Northern hemisphere and June, July, August in the Southern hemisphere).

https://doi.org/10.5194/gmd-2021-2
Preprint. Discussion started: 11 March 2021

Geoscientific Model Development Discussions
Open Access
EGU

Despite the model displaying average temperature biases across some regions of up to ~3K, there is no consistent relationship between such biases and the model's ability to correctly simulate year-to-year variability (Figure 7). More than half of the year-to-year variability is captured by ~60% of the simulated grid cells (Figure 8). Squared Pearson's product moment correlations (R^2) calculated between (i) annual mean SST timeseries at each grid point from the ERA5 forced S2P3R V2.0 simulations and (ii) satellite SST data (Merchant *et al.*, 2019) from 2006-2016 (inclusive) demonstrate high levels of skill in areas such as north of Australia, the Java Sea and the Bering Sea (Figure 7) despite these areas displaying significant positive/negative temperature biases (Figure 4). Conversely, the northern South China sea and southern Australia display low skill at capturing interannual variability (Figure 7), despite the model displaying low temperature biases in these regions (Figure 4). In the case of the South China sea this may relate to highly variable riverine freshwater influences on stratification.

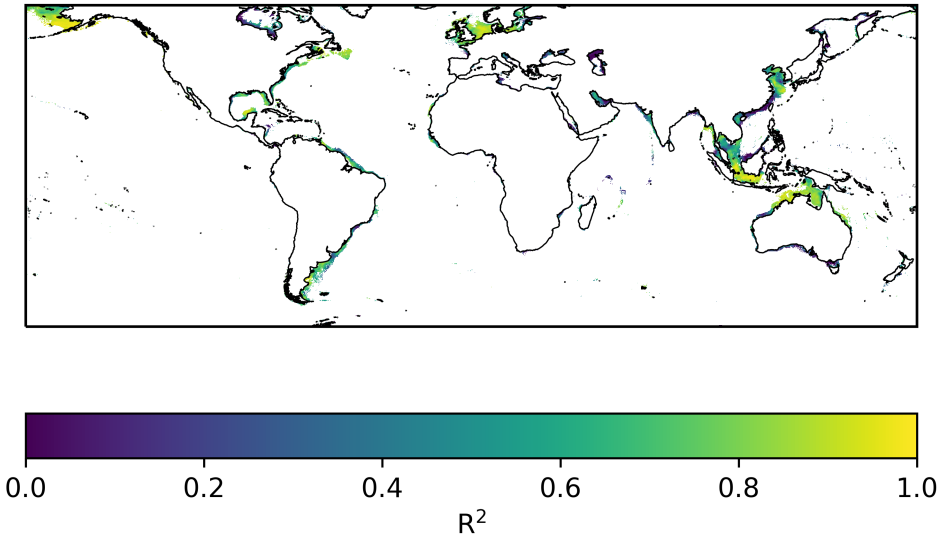

Figure 7. Pearson's R^2 calculated between annual mean Model SST simulation and annual mean satellite SST data (Merchant et al., 2019) between 2006 and 2016.

https://doi.org/10.5194/gmd-2021-2
Preprint. Discussion started: 11 March 2021

Geoscientific Model Development Discussions

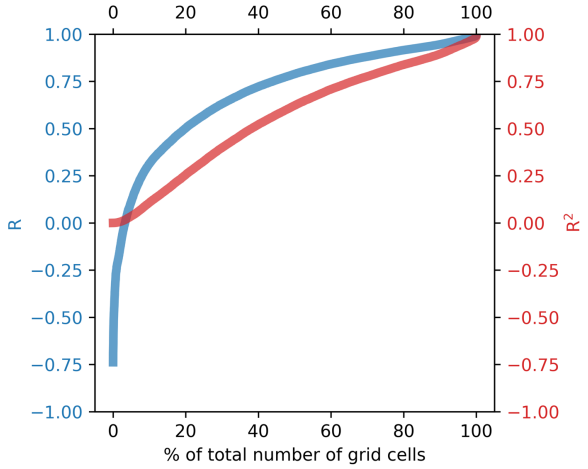

Figure 8. Sorted R and R^2 values from all grid cells calculated from global shelf-sea SST simulation correlation with satellite SST (Figure 7).

5.2 Global Biogeochemical Evaluation

The biological component of S2P3 v2.0 remains unchanged from previous versions, other than through the addition of a spatially varying nutrient field derived from World Ocean Atlas (Levitus, 1982) to which the bottom water nitrate is relaxed. S2P3 has previously been used to investigate biological questions including investigating the drivers of timing of spring blooms in response to stratification (Sharples *et al.*, 2006) and to explore the impact of tidal cycles on productivity (Sharples, 2008) for typical North West European shelf seas. More recently a version of S2P3 has been developed to better represent the impacts of grazing and to include the impact of photo-acclimation on phytoplankton growth (Bahamondes Dominguez *et al.*, 2020).

Evaluation of the model's biological performance at a global scale is more challenging than the evaluation of surface temperature, because satellite chlorophyll-a products are often unreliable in shallow waters, where suspended sediment, coloured dissolved organic matter (CDOM) and bottom reflection influence the retrievals considerably (Darecki and Stramski, 2004). The analysis presented here uses the ESA CCI Chlorophyll-a product data (Sathyendranath *et al.*, 2020) but filters out waters shallower than 70m (Jackson et al., 2019) to avoid the issues mentioned above. The model demonstrates low (<0.2 mg m^{-3}) chlorophyll-a biases when compared to satellite estimates in all regions other Southeast Asia, Australia, the Baltic Sea and the northern Bering Sea (Figure 9). The most extensive area of bias being Southeast Asia and Australia. This is also an area of high SST bias (Figure 4), although there is no strightforward relationship between regoinas of SST and regions of chlorophyll-a bias. Phytoplankton growth in the model is a function of, amongst other factors, temperature and Photosynthetically Active Radiation (PAR). Overestimation of chlorophyll-a may therefore be a response to postive seawater temperature biases, or both may be responding to a positive shortwave radiation bias.

https://doi.org/10.5194/gmd-2021-2
Preprint. Discussion started: 11 March 2021

Geoscientific Model Development Discussions
Open Access
EGU

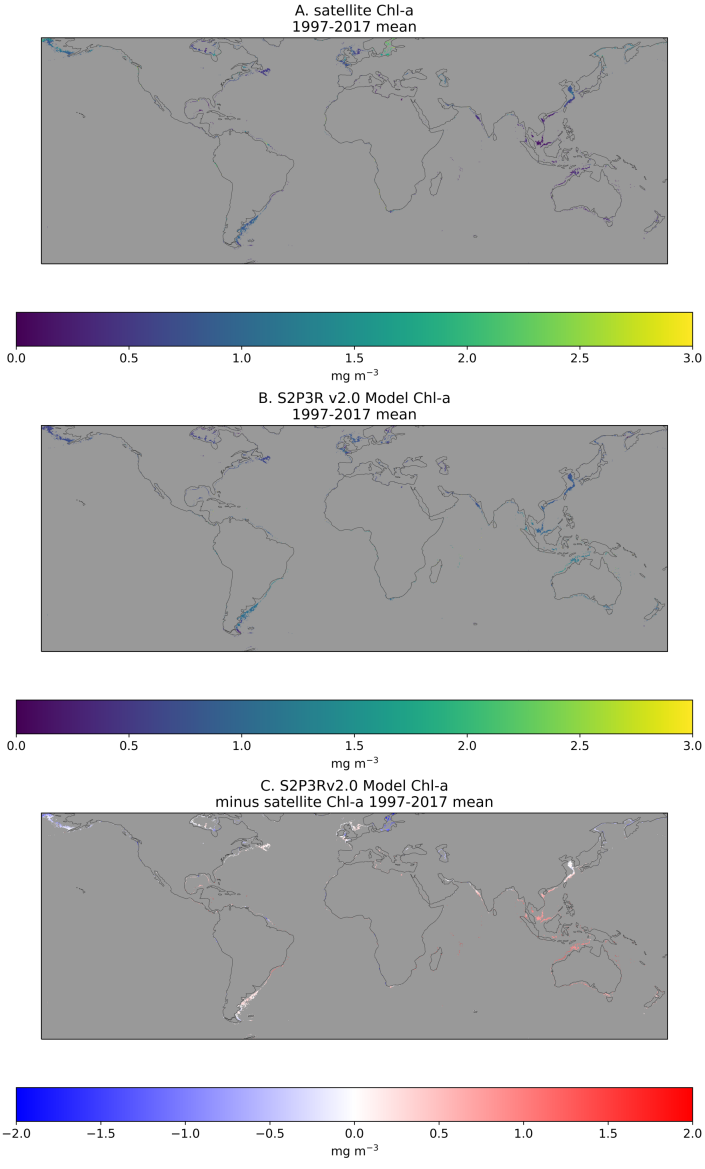

1

https://doi.org/10.5194/gmd-2021-2
Preprint. Discussion started: 11 March 2021

Geoscientific Model Development Discussions

Figure 9. Comparison of surface level chlorophyll-a concentrations with satellite based chlorophyll-a estimates (Sathyendranath *et al.*, 2020). Figures present an annual mean of all data available between 1997 and 2017 inclusive. Satellite data filtered to include just case 2 water, i.e. water ≥ 70m water depth (Jackson et al., 2019). The nutrient data to which the water in the model's bottom level was relaxed to is taken from the winter values in World Ocean Atlas for each hemisphere.

To facilitate a more detailed understanding of the model performance, we now evaluate the model in one mid-latitude region, the North West European Shelf, then one lower latitude region, the Great Barrier Reef.

6.1 North West European Shelf Physical Evaluation

The North West European Shelf is both typical of the mid-latitude regions, where the assumptions made in this modelling framework appear to work well (Figure 4), and is a large area of shallow water which has previously been studied in detail both observationally (e.g. Smyth *et al.*, 2015) and using state of the art 3D models (e.g. Graham *et al.*, 2018).

Forced with the ERA5 atmospheric data (Hersbach *et al.*, 2019), S2P3-R v2.0 simulates the time-averaged SST within 0.5K across much of the North West European Shelf (Figure 10). The model also simulates the trend and interannual variability in SST well in the North Sea, English Channel and Irish Sea (Figure 11), despite the North Sea and English Channel displaying cool and warm temperature biases of approximately 0.5K respectively (Figure 11). The cool bias in the northern North Sea is consistent with the model not accounting for the inflow of relatively warm Atlantic Water via the Dooley Current between Orkney and Shetland (Dooley, 1974; Marsh *et al.*, 2017; Sheehan *et al.*, 2020).

https://doi.org/10.5194/gmd-2021-2
Preprint. Discussion started: 11 March 2021

Geoscientific Model Development Discussions
Open Access
EGU

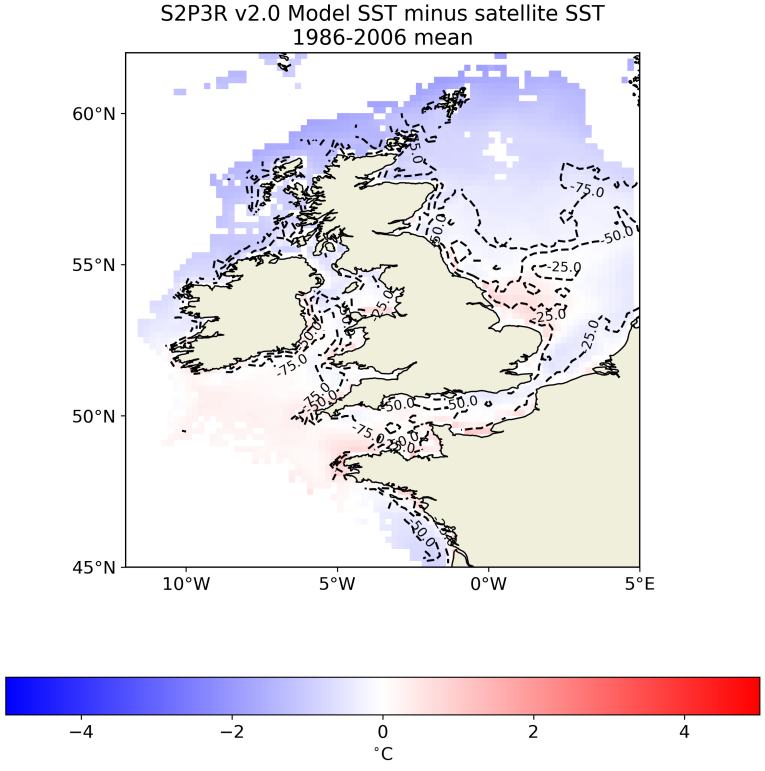

Figure 10. S2P3R v2.0 SST averaged between the years 1986 and 2006 inclusive minus satellite SSTs (Merchant et al., 2019) averaged over the same interval. Labelled dashed lines illustrate bathymetry in meters.

https://doi.org/10.5194/gmd-2021-2
Preprint. Discussion started: 11 March 2021

Geoscientific Model Development Discussions
Open Access
EGU

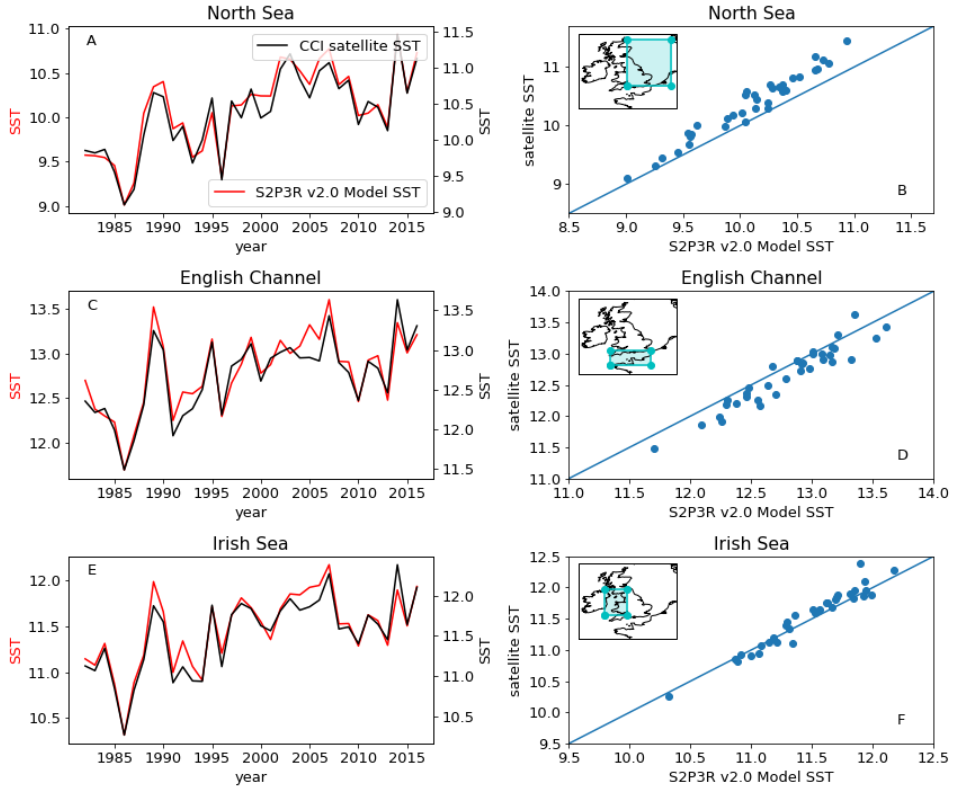

Figure 11. S2P3R v2.0 SST averaged annually and across the three regions highlighted in inset maps, and annually averaged satellite SSTs (Merchant et al., 2019) from the same regions.

Bottom water temperatures can be examined at individual locations using mooring data, as done in Marsh et al., (2015), or at sparse locations against gridded data (e.g. Good, Martin and Rayner, 2013), but to facilitate a more spatially complete assessment we here turn to state-of-the-art model output, generated by the 1.5km NEMO-shelf Atlantic Margin Model (AMM15) (Graham *et al.*, 2018). We find that S2P3-R v2.0 replicates the average values and interannual variability in bottom water temperatures in the North Sea, English Channel and Irish sea captured by the AMM15 model (Graham *et al.*, 2018) with biases of less than 0.5K and R^2 values of 0.92, 0.84 and 0.93 the North Sea, English Channel and Irish Sea respectively (Figure 12). While the AMM15 model is not a perfect surrogate for observations, this comparison gives us confidence in these regions that the use of the highly computationally efficient S2P3-R v2.0 model to a first order gives us comparable bottom water temperature results to a state-of-the-art and computationally demanding three-dimensional modelling system.

https://doi.org/10.5194/gmd-2021-2
Preprint. Discussion started: 11 March 2021

Geoscientific Model Development Discussions

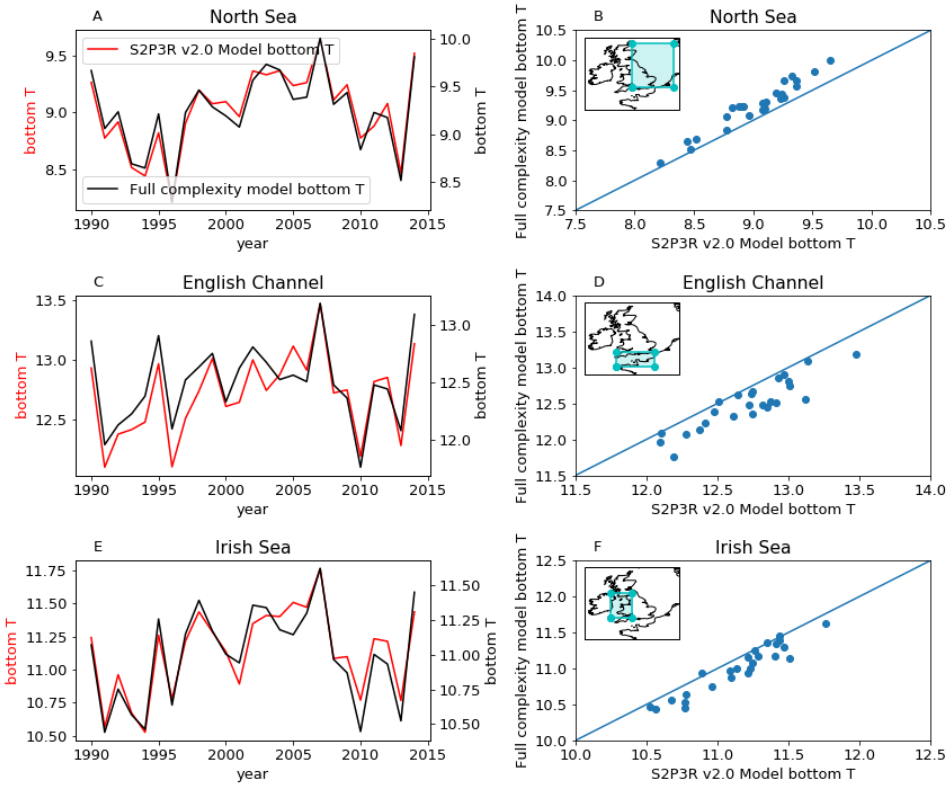

Figure 12. S2P3R v2.0 bottom water temperatures averaged annually and across the three regions highlighted in inset maps, and annually bottom water temperatures from these same regions taken from a state-of-the art shelf sea model hindcast (Graham et al., 2018).

6.2 North West European Shelf Biogeochemical Evaluation

https://doi.org/10.5194/gmd-2021-2
Preprint. Discussion started: 11 March 2021

Geoscientific Model Development Discussions
Open Access
EGU

S2P3R v2.0 underestimates surface chlorophyll-a when compared to annual mean satellite derived estimates (Sathyendranath *et al.*, 2020) across most of the North West European Shelf by 0.25 to 0.50 mg/m^3 (Figure 13). The smallest bias is seen in the North Sea, and the largest in the Irish Sea (Figure 13).

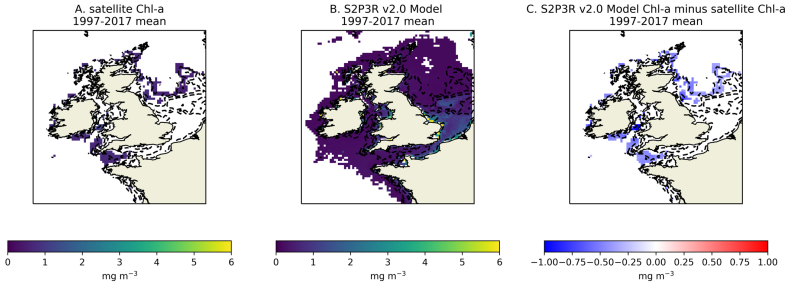

Figure 13. Comparison of North West European Shelf surface level chlorophyll-a concentrations with satellite based chlorophyll-a estimates (Sathyendranath et al., 2020). Figures present an annual mean of all data available between 1997 and 2017 inclusive. Dashed lines represent 20m depth contours. Satellite data are filtered to include just case 2 water, i.e. water ≥ 70m water depth (Jackson et al., 2019).

The seasonal and interannual variability of phytoplankton production, and therefore chlorophyll-a concentration are strongly influenced by changes in stratification. Where the water column is mixed throughout the year (e.g English channel and southern North Sea), phytoplankton growth tends to display a single peak governed to a first order by the cycle of solar irradiance and the availability of nutrients, with development of the peak slowed by mixing of phytoplankton into deeper, poorly lit, waters (e.g. Figure 14 a, c, e, g, i, j) (Wafar, Le Corre and Birrien, 1983). Where the water column is seasonally stratified and winter mixing has removed any upper-water column nutrient limitation potential, a spring bloom typically develops as the mixed layer - defined by turbulence levels (Chiswell, 2011; Chiswell, Calil and Boyd, 2015) - shallows across a seasonally-deepening critical depth, shallower than which light-limited phytoplankton production exceeds approximately depth-invariant phytoplankton losses (Sverdrup, 1953). In these seasonally stratified waters, an autumn bloom (and therefore second chlorophyll-a peak) may also develop as cooling results in buoyancy loss from the surface or winds increase turbulence, and the mixed layer deepens and refreshes what have become nutrient limited sunlit waters, with nutrients from deeper in the water column (Findlay *et al.*, 2006). This potentially skewed, bimodal distribution is captured by the model in seasonally stratified sites (Figure 14, c, k, o). While in the central North Sea and Celtic Sea, the seasonal evolution of model chlorophyll-a concentrations match closely with that inferred from observations (Figure 14 c, k, o), in most sites the model fails to capture the full complexity of the seasonal signal. The model also fails to capture the interannual variability in chlorophyll-a at those sites where long enough observational timeseries exist to assess this (Figure 14). The lack of evidence for correctly simulated interannual variability potentially reflects the importance of processes not represented in this model such as photo-acclimation (Bahamondes Dominguez *et al.*, 2020), grazing (Bahamondes Dominguez *et al.*, 2020) and phytoplankton species composition (Barnes *et al.*, 2015) in controlling interannual variability, or the importance of variability in nutrient flux across the shelf-break (Holt *et al.*, 2012) and from rivers (Capuzzo *et al.*, 2018).

https://doi.org/10.5194/gmd-2021-2
Preprint. Discussion started: 11 March 2021

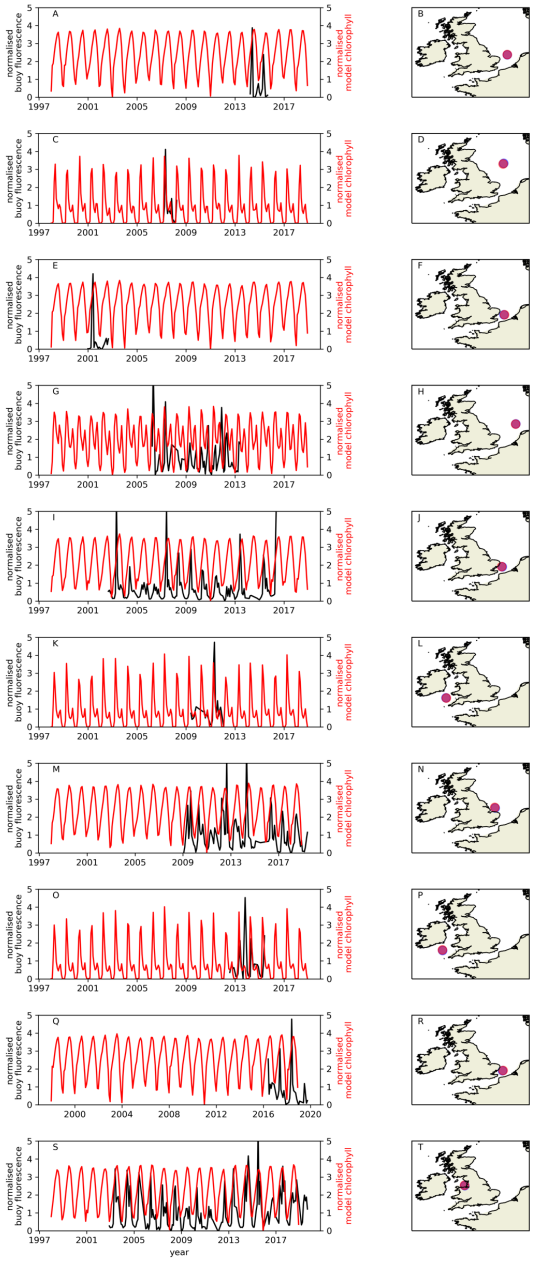

Figure 14 Comparison of model chlorophyll-a timeseries (red) with chlorophyll-a fluoresence measurements (black) made on 10 autonomous buoys situated round the UK as part of the CEFAS SmartBuoy network (Sivyer, 2016). Both datasets have been monthly averaged and normalised by their standard deviation. Fluoresence data has been filtered

https://doi.org/10.5194/gmd-2021-2
Preprint. Discussion started: 11 March 2021

Geoscientific Model Development Discussions
Open Access
EGU

to include only that collected between 18:00 and 06.00 hours to avoid quenching of the signal by sunlight. Maps on the right hand side illustrate the location of each buoy. Note that buoys have been operational over different time windows.

7.1 Great Barrier Reef Physical Evaluation

Moving to the low-latitudes where SST biases in the S2P3R v2.0 model are typically larger than they are in the mid-latitudes (Figure 4), a simulation has been undertaken which encompasses the Great Barrier Reef (GBR). The GBR is well instrumented, allowing analysis of subsurface as well as surface temperatures in this region.

The modelled SSTs in the GBR display a positive bias relative to satellite SSTs in the north and negative bias in the south (Figure 15). This may relate to the fact that the model does not simulate lateral advection, which will be exporting heat from the north to the south in the East Australian Current.

S2P3R v2.0 appears to capture much of the interannual variability observed in SSTs over the GBR since the early 1980s (Figure 16), but with a temperature bias of <0.5K (Figure 15). The simulation however appears to erroneously simulate a stepwise cooling around the year 2000 which compromises the overall correlation between model and satellite SSTs (Figure 16). This stepwise cooling may reflect changes in the assimilation of observations into the ERA5 reanalysis product which is used to force the model.

https://doi.org/10.5194/gmd-2021-2
Preprint. Discussion started: 11 March 2021

Geoscientific Model Development Discussions
Open Access
EGU

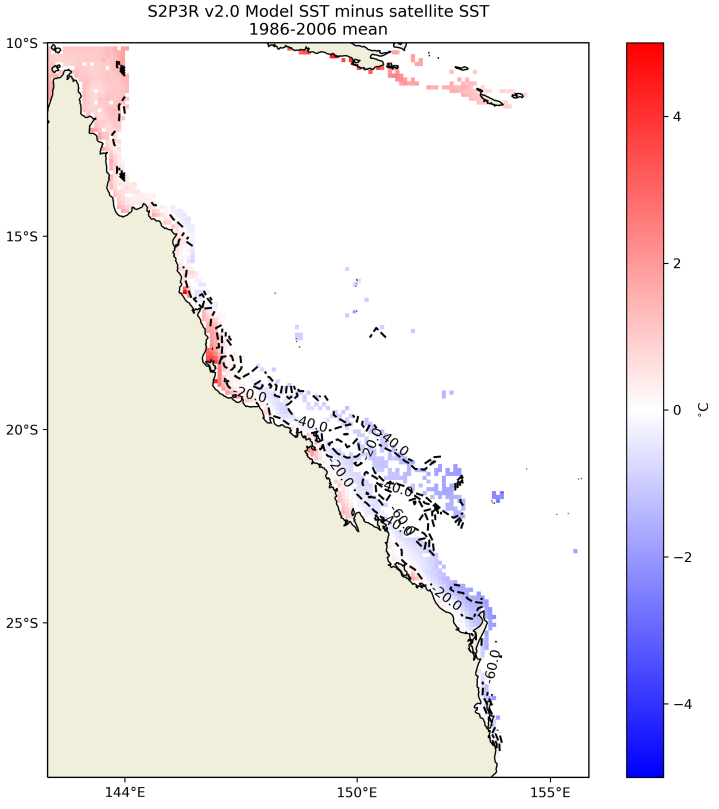

Figure 15. S2P3R v2.0 SST averaged between 1986 and 2006 inclusive minus satellite SSTs (Merchant et al., 2019) over the same interval. Labelled dashed lines show bathymetry in meters.

https://doi.org/10.5194/gmd-2021-2
Preprint. Discussion started: 11 March 2021

Geoscientific Model Development Discussions
Open Access
EGU

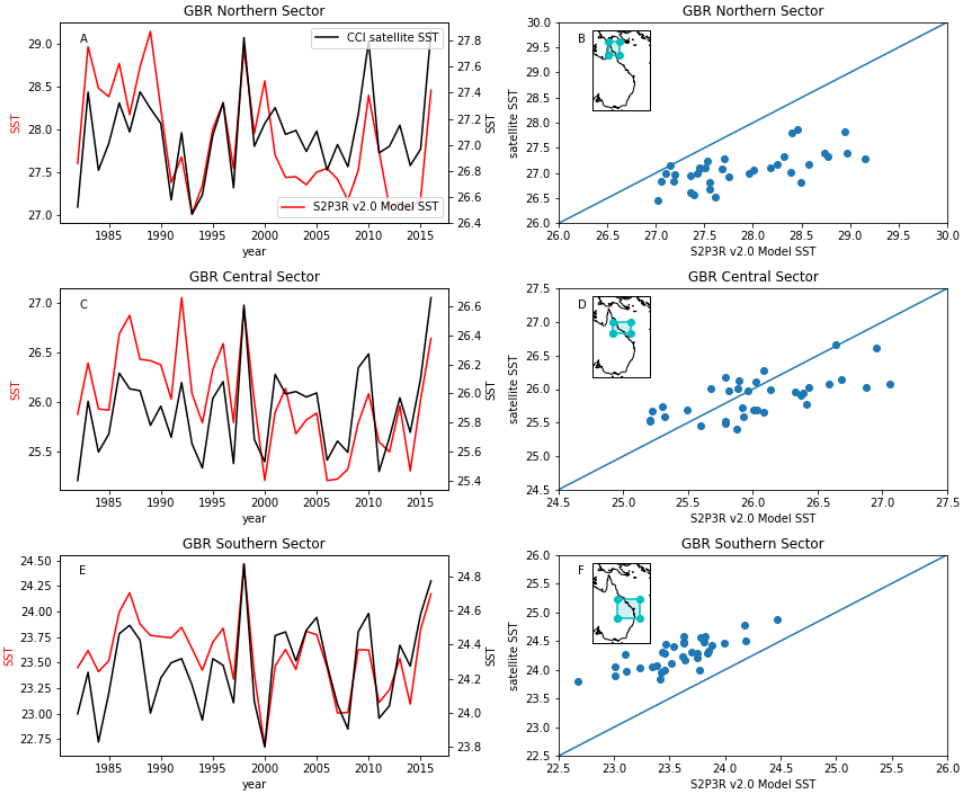

Figure 16. Comparison of interannual SST variability between S2P3R v2.0 and satellite (Merchant et al., 2019) over the GBR, subdivided into three latitudinally delineated regions. These regions are identified in the inset maps.

While a state-of-the-art regional model for the GBR region exists (Steven et al., 2019), a long validated hindcast is not available to allow evaluation of the S2P3R V2.0 simulation of bottom water temperatures in the GBR analogous to that presented here for the North West European Shelf. The GBR is however instrumented with an extensive mooring network, making up part of the IMOS FAIMMS (Integrated Marine Observing System, Facility for Automated Intelligent Monitoring of Marine Systems) Sensor Network (IMOS, 2009a, 2009b, 2009d, 2009e, 2009c, 2015, 2017). The location of the moorings utilised in the evaluation presented here are highlighted in Figure 17.

In situ observations indicate that a cool bias exists in the modelled SSTs, but this is restricted to austral winter months (Figure 17c). The fact that a warm bias is not evident in the mooring data, as it is in the satellite SST data (Figure 15), may result from a sampling bias within the mooring dataset towards deeper waters. Modelled bottom water temperatures from the lower latitude mooring sites present a cool bias, but a linear relationship when compared with observational data (Figure 17d). The cool bias may reflect the fact that the model output against which the observations are compared represent a mean value across a ~10km^2 grid-cell and for example may well therefore not be simulating the conditions at the same depth as the observations are made.

https://doi.org/10.5194/gmd-2021-2
Preprint. Discussion started: 11 March 2021

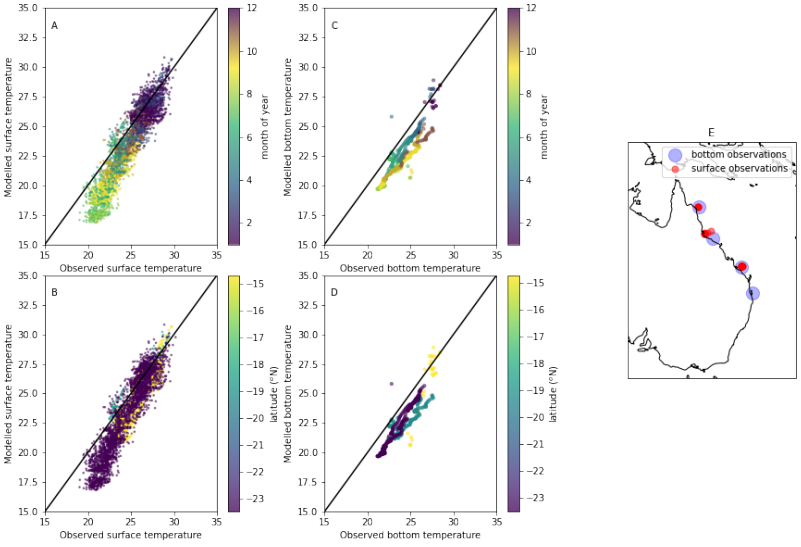

Figure 17. Comparison of S2P3R v2.0 surface (A and B) and bottom (C and D) temperatures against mooring observations from IMOS and FAIMMS and moorings (IMOS, 2009a, 2009b, 2009d, 2009e, 2009c, 2015, 2017). The x-y values of the data presented in plots on the top and bottom (A and B, and C and D) are identical, but are coloured to highlight where temporal and geographical biases exist in the model output. Seabed observations are considered here to be those falling within 5m of the site-depth for each mooring. The map shows the location of surface (red) and bottom (blue) temperature mooring observations used in model evaluation over the GBR.

7.2 Great Barrier Reef Biogeochemical Evaluation

In GBR case 2 water, i.e. water ≥ 70m water depth (Jackson et al., 2019), where comparison with the European Space Agency Climate Change Initiative (ESA CCI) long term satellite chlorophyll data (Sathyendranath et al., 2020) is meaningful, the S2P3R v2.0 simulation of chlorophyll displays low negative biases <0.2 mg/m^3 (Figure 18). These biases are considerably lower than those simulated on the North West European shelf (Figure 13), the region within which the model was originally designed to investigate chlorophyll seasonality (Sharples *et al.*, 2006).

https://doi.org/10.5194/gmd-2021-2
Preprint. Discussion started: 11 March 2021

Geoscientific Model Development Discussions
Open Access
EGU

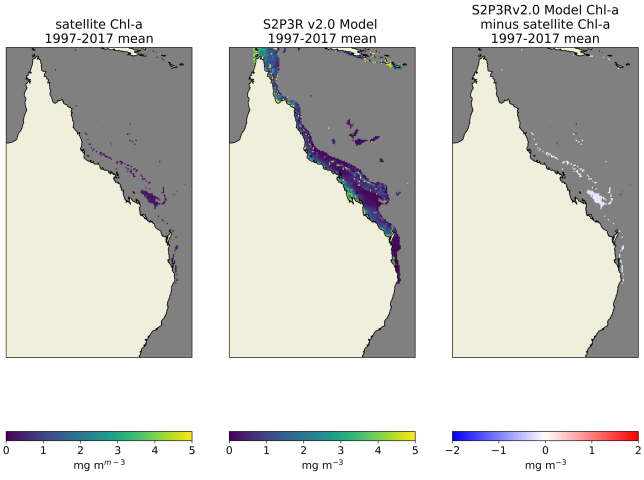

Figure 18. Comparison of GBR surface level chlorophyll-a concentrations with satellite based chlorophyll-a estimates (Sathyendranath *et al.*, 2020). Figures present an annual mean of all data available between 1997 and 2017 inclusive. Satellite data filtered to include just case 2 water, i.e. water ≥ 70m water depth (Jackson et al., 2019).

Evaluation of the model's ability to simulate the seasonal cycle and interannual variability in chlorophyll-a in the GBR region has been conducted using moored buoy fluorescence data, as done for the North West European Shelf, but with more restricted temporal coverage (Figure 19). Unlike the spring/autumn bloom dominated seasonal evolution of chlorophyll-a experienced in many temperate sites, the seasonal cycle simulated by the model and illustrated by the observations across the GBR sites examined here follows a relatively smooth oscillation with the peak values in the model data occurring in late summer (Figure 19). In contrast to many of the North West European Shelf sites, this behaviour likely results from the intersection of the critical depth (Sverdrup, 1953) with the seabed at these high light and shallow locations. The incomplete or short length of the GBR fluorescence observational datasets mean that it is not possible to undertake a detailed investigation of interannual variability, however the longest of the mooring datasets (Figure 19k) exhibits its lowest chlorophyll-a peaks in the same years as those simulated by the model (2018 and 2019). In a typically oligotrophic setting, like much of the GBR, one might expect year to year variability to be dominated by injections of nutrients from the shelf-break or the coast (Furnas and Mitchell, 1986). Despite the model not representing these processes, it never-the-less simulates considerable inter-annual variability, indicating the potential for atmospheric and vertical ocean dynamics drivers of such variability.

https://doi.org/10.5194/gmd-2021-2
Preprint. Discussion started: 11 March 2021

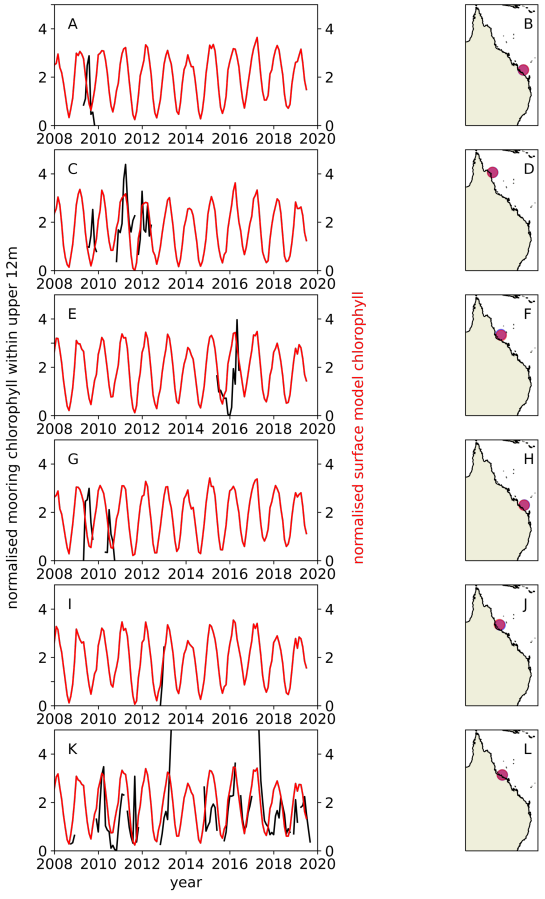

Figure 19. Comparison of model chlotophyll-a timeseries (red) with chlorophyll-a fluoresence measurements (black) made on 6 moored buoys situated down the GBR as part of the IMOS Australian National Mooring Network (IMOS, 2015). Both datastes have been monthly averaged and normalised by their standard deviation. Surface level data was not available for all sites, so data represent an average over the top 12m of the water column to improve spatial data coverage.

8. Summary and discussion:

Forced by observation-derived atmospheric conditions, a simulation spanning the shelf seas of the global tropical-to-subpolar ocean at approximately 10km^2 resolution captures >50% of the observed interannual SST variability between 2006 and 2016 in ~60% of the grid cells, and greater than 80% of the interannual SST variability in ~20% of the grid cells (Figure 8). This tells us that a large part of the SST variability in a significant component of our global shelf-seas is atmospherically forced, rather than being forced by variable lateral exchanges with the deep ocean or runoff. When compared to satellite data (Merchant *et al.*, 2019), 61% of grid cells however present an SST bias of greater than 1K and 42% present an SST bias of greater than 2K, highlighting limitations to the simple modelling approach.

https://doi.org/10.5194/gmd-2021-2
Preprint. Discussion started: 11 March 2021

Together, analysis of SST variability and SST bias indicate there are significant areas of our global shelf seas where the model should be used with extreme caution. These regions are likely to be those which have; (1) substantial exchange of heat with the open ocean through lateral advection, (2) low tidally driven mixing and therefore a low ratio of vertical/horizontal control over SSTs (Figure 5), (3) significant influences from local processes/properties such as riverine inputs or locally unusual bottom drag coefficients, (4) high salinity variability and low temperatures, or (5) on-shelf propagation and dissipation of the internal tide. The model could however be tuned to account for some of these influences if studies were to be undertaken with a focus on such regions.

Regional evaluation has been conducted across the North West European Shelf around the UK, and the Great Barrier Reef. The model captures most of the observed SST trend and variability in the waters around the UK (Figure 11), with a temperature biases of <0.5K across most of the region (Figure 10). S2P3R v2.0 also captures between 84 and 93% of the variability in bottom water temperatures simulated by a state-of-the-art shelf sea model hindcast (Graham *et al.*, 2018) for the three focal regions of the North Sea, English Channel and Irish Sea. Comparison of modelled and satellite SSTs across the Great Barrier Reef indicate over ~10-year intervals the model performs well, but there appear to be step-changes in the modelled SST which are not seen in the satellite data. The discontinuity occurring around the year 2000 may reflect a step change in the data assimilation configuration used within the ERA5 product or data being assimilated by that product (Hersbach *et al.*, 2018) used to provide the atmospheric forcing to S2P3R v2.0. Alternatively, the step changes may result from changes in the lateral supply of heat from the open ocean.

A particular strength of this modelling approach is likely to be in examining or predicting anomalies or extremes which occur under a consistent set of oceanographic conditions. For example, the marine heat waves associated with tropical coral bleaching tend to occur following doldrum-like condition, when there is limited advection and mixing (Skirving, Heron and Heron, 2011).

Observational limitations mean the model's simulation of biological production in space and time is harder to assess than that of temperature. The model however captures the broad scale patterns of surface chlorophyll (Figure 9, Figure 13, Figure 18), with a weak indication of latitudinally varying bias towards overprediction in low latitudes and underprediction in high latitudes (Figure 9). The model displays considerable skill in many locations at simulating intra-annual chlorophyll variability (Figure 14, Figure 19), but no demonstrable skill at simulating inter-annual chlorophyll variability. This implies that the large-scale processes which govern the seasonal progression of primary production do not also govern interannual variability. Factors such as riverine input of nutrients may dominate interannual variability in many locations (Lenhart, Radach and Ruardij, 1997). These results emphasise the importance of decadal and longer observational biogeochemical timeseries for assessing the skill of models at simulating those processes which are likely to govern the biogeochemical response of our shelf seas to anthropogenic climate change.

In summary, S2P3R v2.0 is a simple to use, computational efficient shelf sea modelling tool ideally suited to (a) semi-dynamically downscaling climate projections, (b) undertaking large-scale, long or large ensemble projections, (c) use by management or policy groups without access to large technical or computational resources.

https://doi.org/10.5194/gmd-2021-2
Preprint. Discussion started: 11 March 2021

The objective assessment of the model presented here will hopefully guide potential users as to whether S2P3R v2.0 is the tool to answer their questions. Where S2P3R v2.0 is considered to be an appropriate tool, we would encourage local assessment of the data presented here at a global scale and hope to facilitate this through the provision of these data (see Data Availability section). Finally, within the Code Availability section of this manuscript we provide the model code, code required to produce the model forcing datasets, an example model setup with pre-prepared forcing data, and within the Readme file, step-by-step instructions for setting up and running the model.

9. Code Availability

S2P3Rv2.0 is available from github: https://github.com/PaulHalloran/S2P3Rv2.0

The release associated with this manuscript (https://github.com/PaulHalloran/S2P3Rv2.0/releases/tag/v1.0.1) has been archived to Zenodo with the following DOI 10.5281/zenodo.4147559.

The README file available on github or via the DOI link provides step by step instructions for how to install, setup and run the model, and provides a basic script for analysing the model output. At the bottom of the README a worked example is provided to help the user go through the full process from generating model forcing files, running the model and displaying the output with some example data.

10. Data availability

Model minus satellite SST data from the global (65°S-65°N) simulation averaged between 2006 and 2016 from which the global validation has been undertaken in this manuscript are archived as netCDF and CSV files to allow potential users to undertake bespoke assessment of the model http://doi.org/10.5281/zenodo.4018815 (Halloran, 2020).

11. Competing interests

The authors declare that they have no conflict of interest.

12. Author contribution

The model development was undertaken by PH. PH lead the analysis with contributions from JMW, BN, RM and WS. All authors contributed to the writing of the manuscript.

13. Acknowledgements

Paul Halloran was supported by the UK Research Council grant NE/V00865X/1. Paul Halloran and Jennifer McWhorter were supported by the QUEX Institute, a University of Exeter and University of Queensland Partnership. This project has received funding from the European Union's Horizon 2020 research and innovation programme under grant agreement No 820989 (project COMFORT, Our common future ocean in the Earth system – quantifying coupled cycles of carbon, oxygen, and nutrients for determining and achieving safe

https://doi.org/10.5194/gmd-2021-2
Preprint. Discussion started: 11 March 2021

operating spaces with respect to tipping points). This manuscript reflects only the authors' views; the European Commission and their executive agency are not responsible for any use that may be made of the information the work contains. William Skirving was supported by NOAA grant NA19NES4320002 (Cooperative Institute for Satellite Earth System Studies) at the University of Maryland/ESSIC. The scientific results and conclusions, as well as any views or opinions expressed herein, are those of the author(s) and do not necessarily reflect the views of NOAA or the Department of Commerce. The Smartbuoy data was made available by Cefas and funded by Defra and the UK Research Council Candyfloss and Celtic Deep 2 grant NE/K001957/1. The IMOS buoy data was provided by the IMOS Queensland and Northern Australian Moorings sub-facility of the Australian National Mooring Network funded by the Australian Institute of Marine Science and the Integrated Marine Observing System (IMOS)—IMOS is enabled by the National Collaborative Research Infrastructure Strategy (NCRIS), supported by the Australian Government. It is operated by a consortium of institutions as an unincorporated joint venture, with the University of Tasmania as Lead Agent. www.imos.org.au.

Bibliography

Amante, C. and Eakins, B. W. (2009) 'ETOPO1 1 Arc-Minute Global Relief Model: Procedures, Data Sources and Analysis', *NOAA Technical Memorandum NESDIS NGDC-24*. doi: 10.1594/PANGAEA.769615.

Bahamondes Dominguez, A. *et al.* (2020) 'Constraining the response of phytoplankton to zooplankton grazing and photo-acclimation in a temperate shelf sea with a 1-D model - towards S2P3 v8.0', *Geoscientific Model Development Discussions*. doi: 10.5194/gmd-2019-345.

Barnes, M. K. *et al.* (2015) 'Temporal variability in total, micro- and nano-phytoplankton primary production at a coastal site in the Western English Channel', *Progress in Oceanography*. doi: 10.1016/j.pocean.2015.04.017.

Beaman, R. (2010) *Project 3DGBR: a high-resolution depth model for the Great Barrier Reef and Coral Sea*.

Booth, B. B. B. *et al.* (2012) 'Erratum: Aerosols implicated as a prime driver of twentieth-century North Atlantic climate variability (Nature (2012) 484 (228-232))', *Nature*, 485(7399). doi: 10.1038/nature11138.

Bowen, B. W. *et al.* (2016) 'Comparative phylogeography of the ocean planet', *Proceedings of the National Academy of Sciences of the United States of America*. doi: 10.1073/pnas.1602404113.

Canuto, V. M. *et al.* (2001) 'Ocean turbulence. Part I: One-point closure model-momentum and heat vertical diffusivities', *Journal of Physical Oceanography*. doi: 10.1175/1520-0485(2001)031<1413:OTPIOP>2.0.CO;2.

Capuzzo, E. *et al.* (2018) 'A decline in primary production in the North Sea over 25 years, associated with reductions in zooplankton abundance and fish stock recruitment', *Global Change Biology*. doi: 10.1111/gcb.13916.

Chen, T., Rossow, W. B. and Zhang, Y. (2000) 'Radiative effects of cloud-type variations', *Journal of Climate*. doi: 10.1175/1520-0442(2000)013<0264:REOCTV>2.0.CO;2.

Chiswell, S. M. (2011) 'Annual cycles and spring blooms in phytoplankton: Don't abandon Sverdrup completely', *Marine Ecology Progress Series*. doi: 10.3354/meps09453.

Chiswell, S. M., Calil, P. H. R. and Boyd, P. W. (2015) 'Spring blooms and annual cycles of phytoplankton: A unified perspective', *Journal of Plankton Research*. doi: 10.1093/plankt/fbv021.

Darecki, M. and Stramski, D. (2004) 'An evaluation of MODIS and SeaWiFS bio-optical algorithms in the Baltic Sea', *Remote Sensing of Environment*. doi: 10.1016/j.rse.2003.10.012.

Donner, S. D. *et al.* (2005) 'Global assessment of coral bleaching and required rates of adaptation under climate change', *Global Change Biology*. doi: 10.1111/j.1365-2486.2005.01073.x.

Dooley, H. D. (1974) 'Hypotheses concerning the circulation of the northern North Sea', *ICES*

https://doi.org/10.5194/gmd-2021-2
Preprint. Discussion started: 11 March 2021

Journal of Marine Science. doi: 10.1093/icesjms/36.1.54.
Egbert, G. D. and Erofeeva, S. Y. (2002) 'Efficient inverse modeling of barotropic ocean tides', *Journal of Atmospheric and Oceanic Technology*. doi: 10.1175/1520-0426(2002)019<0183:EIMOBO>2.0.CO;2.
Findlay, H. S. *et al.* (2006) 'Modelling of autumn plankton bloom dynamics', *Journal of Plankton Research*. doi: 10.1093/plankt/fbi114.
Furnas, M. J. and Mitchell, A. W. (1986) 'Phytoplankton dynamics in the central Great Barrier Reef-I. Seasonal changes in biomass and community structure and their relation to intrusive activity', *Continental Shelf Research*. doi: 10.1016/0278-4343(86)90078-6.
Good, S. A., Martin, M. J. and Rayner, N. A. (2013) 'EN4: Quality controlled ocean temperature and salinity profiles and monthly objective analyses with uncertainty estimates', *Journal of Geophysical Research: Oceans*. doi: 10.1002/2013JC009067.
Graham, J. A. *et al.* (2018) 'AMM15: A new high-resolution NEMO configuration for operational simulation of the European north-west shelf', *Geoscientific Model Development*. doi: 10.5194/gmd-11-681-2018.
Halloran, P. (2020) *S2P3Rv2.0 bias data [Data set]*, *Zenodo*. doi: zenodo.4018815.
Haywood, J. and Boucher, O. (2000) 'Estimates of the direct and indirect radiative forcing due to tropospheric aerosols: A review', *Reviews of Geophysics*. doi: 10.1029/1999RG000078.
Hersbach, H. *et al.* (2018) 'Operational global reanalysis: progress, future directions and synergies with NWP including updates on the ERA5 production status', *ERA Report Series*. doi: 10.21957/tkic6g3wm.
Hersbach, H. *et al.* (2019) 'Global reanalysis: goodbye ERA-Interim, hello ERA5', *ECMWF Newsletter*. doi: 10.21957/vf291hehd7.
Holt, J. *et al.* (2009) 'Modelling the global coastal ocean', *Philosophical Transactions of the Royal Society A: Mathematical, Physical and Engineering Sciences*. doi: 10.1098/rsta.2008.0210.
Holt, J. *et al.* (2012) 'Oceanic controls on the primary production of the northwest European continental shelf: Model experiments under recent past conditions and a potential future scenario', *Biogeosciences*. doi: 10.5194/bg-9-97-2012.
Van Hooidonk, R. *et al.* (2016) 'Local-scale projections of coral reef futures and implications of the Paris Agreement', *Scientific Reports*. doi: 10.1038/srep39666.
IMOS (2009a) *GBRHIS: Heron Island South Shelf Mooring component of the GBR Mooring Array*.
IMOS (2009b) *GBRLSH: Lizard Island Shelf Mooring component of the GBR Mooring Array*.
IMOS (2009c) *GBROTE: One Tree Island Shelf Mooring component of the GBR Mooring Array*.
IMOS (2009d) *GBRPPS: Palm Passage Shelf Mooring component of the GBR Mooring Array*.
IMOS (2009e) *Northern Australia Automated Marine Weather and Oceanographic Stations, Sites: [Yongala Mooring (NRSYON)]*.
IMOS (2015) *Integrated Marine Observing System (IMOS). Facility for the Automated Intelligent Monitoring of Marine Systems - FAIMMS*. Available at: https://apps.aims.gov.au/metadata/view/d63dc150-0d02-11dd-bbbb-00008a07204e.
IMOS (2017) *IMOS - ANMN National Reference Station (NRS) Ningaloo Mooring (NRSNIN)*.
Jackson, T. *et al.* (2019) *Ocean Colour Climate Change Initiative Product User Guide D3.4 PUG*. Available at: https://esa-oceancolour-cci.org/sites/esa-oceancolour-cci.org/alfresco.php?file=a68aa514-3668-4935-9235-fca10f7e8bee&name=OC-CCI-PUG-v4.1-v1.pdf.
Kwiatkowski, L. *et al.* (2014) 'What spatial scales are believable for climate model projections of sea surface temperature?', *Climate Dynamics*, 43(5–6). doi: 10.1007/s00382-013-1967-6.
Lenhart, H. J., Radach, G. and Ruardij, P. (1997) 'The effects of river input on the ecosystem dynamics in the continental coastal zone of the North Sea using ERSEM', *Journal of Sea Research*. doi: 10.1016/S1385-1101(97)00049-X.
Levitus, S. (1982) 'Climatological Atlas of the World Ocean', *NOAA Professional Paper 13, U.S. Gov. Printing Office, Rockville, M.D.*, p. 190.
Marsh, R. *et al.* (2017) 'Large-scale forcing of the European Slope Current and associated inflows to the North Sea', *Ocean Science*. doi: 10.5194/os-13-315-2017.
Marsh, R., Hickman, A. E. and Sharples, J. (2015) 'S2P3-R (v1.0): A framework for efficient regional modelling of physical and biological structures and processes in shelf seas', *Geoscientific Model*

Development. doi: 10.5194/gmd-8-3163-2015.
Merchant, C. J. *et al.* (2019) 'Satellite-based time-series of sea-surface temperature since 1981 for climate applications', *Scientific data*. doi: 10.1038/s41597-019-0236-x.
van der Molen, J., Ruardij, P. and Greenwood, N. (2017) 'A 3D SPM model for biogeochemical modelling, with application to the northwest European continental shelf', *Journal of Sea Research*. doi: 10.1016/j.seares.2016.12.003.
Mora, C. *et al.* (2013) 'Biotic and Human Vulnerability to Projected Changes in Ocean Biogeochemistry over the 21st Century', *PLoS Biology*, 11(10). doi: 10.1371/journal.pbio.1001682.
Sathyendranath, S. *et al.* (2020) 'ESA Ocean Colour Climate Change Initiative (Ocean_Colour_cci): Global chlorophyll-a data products gridded on a sinusoidal projection, Version 4.2', *Centre for Environmental Data Analysis*. doi: https://catalogue.ceda.ac.uk/uuid/99348189bd33459cbd597a58c30d8d10.
Sharples, J. *et al.* (2006) 'Inter-annual variability in the timing of stratification and the spring bloom in the North-western North Sea', *Continental Shelf Research*. doi: 10.1016/j.csr.2006.01.011.
Sharples, J. (2008) 'Potential impacts of the spring-neap tidal cycle on shelf sea primary production', *Journal of Plankton Research*. doi: 10.1093/plankt/fbm088.
Sheehan, P. M. F. *et al.* (2020) 'Weekly variability of hydrography and transport of northwestern inflows into the northern North Sea', *Journal of Marine Systems*. doi: 10.1016/j.jmarsys.2019.103288.
Simpson, J. H. and Sharples, J. (2012) *Introduction to the Physical and Biological Oceanography of Shelf Seas*, *Introduction to the Physical and Biological Oceanography of Shelf Seas*. doi: 10.1017/cbo9781139034098.
Sivyer (2016) *Cefas SmartBuoy Monitoring Network*. doi: doi: https://doi.org/10.14466/CefasDataHub.10.
Skirving, W., Heron, M. and Heron, S. (2011) 'The hydrodynamics of a bleaching event: Implications for management and monitoring', in. doi: 10.1029/61ce09.
Smith, S. D. and Banke, E. G. (1975) 'Variation of the sea surface drag coefficient with wind speed', *Quarterly Journal of the Royal Meteorological Society*. doi: 10.1002/qj.49710142920.
Smyth, T. *et al.* (2015) 'The Western Channel Observatory', *Progress in Oceanography*. doi: 10.1016/j.pocean.2015.05.020.
Song, H. *et al.* (2011) 'Interannual variability in phytoplankton blooms and plankton productivity over the Nova Scotian Shelf and in the Gulf of Maine', *Marine Ecology Progress Series*. doi: 10.3354/meps09002.
Steven, A. D. L. *et al.* (2019) 'eReefs: An operational information system for managing the Great Barrier Reef', *Journal of Operational Oceanography*. doi: 10.1080/1755876X.2019.1650589.
Sverdrup, H. U. (1953) 'On conditions for the vernal blooming of phytoplankton', *ICES Journal of Marine Science*. doi: 10.1093/icesjms/18.3.287.
Wafar, M. V. M., Le Corre, P. and Birrien, J. L. (1983) 'Nutrients and primary production in permanently well-mixed temperate coastal waters', *Estuarine, Coastal and Shelf Science*. doi: 10.1016/0272-7714(83)90128-2.